APPLIED ORGANOMETALLIC CHEMISTRY
Appl. Organometal. Chem. 2004; **18**: 676–683
Published online in Wiley InterScience (www.interscience.wiley.com). DOI:10.1002/aoc.628

Flash vacuum thermolysis of 3,4-dimethyl-1-germacyclopent-3-enes: UV photoelectron spectroscopic characterization of GeH_2 and $GeMe_2$†

Virginie Lemierre[1], Anna Chrostowska[1]*, Alain Dargelos[1], Patrick Baylère[1], William J. Leigh[2] and Cameron R. Harrington[2]**

[1]Laboratoire de Physico-Chimie Moléculaire, UMR 5624, Université de Pau, Av. de l'Université, BP 1155, 64013 Pau Cedex, France
[2]Department of Chemistry, McMaster University, 1280 Main Street West, Hamilton, Ontario L8S 4M1, Canada

Received 8 February 2004; Revised 19 February 2004; Accepted 2 March 2004

Gas-phase UV photoelectron spectra of germylene (GeH_2) and its dimethyl analogue ($GeMe_2$) have been recorded, using flash vacuum thermolysis of 3,4-dimethyl- and 1,1,3,4-tetramethyl-germacyclopent-3-ene to generate these reactive species in the inlet of the photoelectron spectrometer. The lowest vertical ionization bands for GeH_2 (9.4 eV) and $GeMe_2$ (8.2 and 10.0 eV) have been located with the aid of time-dependent density functional theory calculations carried out at the B3LYP/6-311G(d,p) level of theory. Similar experiments carried out with 3,4-dimethyl-1,1-diphenylgermacyclopent-3-ene, in an attempt to record the photoelectron spectrum of diphenylgermylene ($GePh_2$), were less conclusive, but are consistent with the theoretically predicted lowest lonization potential of 8.0–8.2 eV for $GePh_2$. Photoelectron spectra of the three germacyclopentene derivatives are also reported. Copyright © 2004 John Wiley & Sons, Ltd.

KEYWORDS: germylene; dimethylgermylene; UV photoelectron spectroscopy; ionization potential; quantum mechanical calculation; flash vacuum thermolysis

INTRODUCTION

The synthesis and experimental characterization of the silicon and germanium analogues of methylene (CH_2) and other simple carbenes are a considerable challenge because of their intrinsic kinetic instabilities. The chemistry and spectroscopy of these low-coordinate species have recently been reviewed; for reviews of simple systems, see Refs 1–3. Other, more frequent reviews have covered the synthesis, structures and properties of stable derivatives, which have been much more extensively studied; for recent reviews of stable silylenes and germylenes, see Refs 4–8. Since the reactivities and properties of stabilized derivatives obviously derive ultimately from those of the parent molecules, it remains of great importance to further our understanding of simple systems, devoid of possible perturbing influences due to substituents. Theory is far ahead of experiment in this regard.[9–14]

The structures and reactivities of simple germylenes have been much less extensively characterized than the corresponding silicon analogues.[1–3] The ground-state vibrational frequencies of GeH_2, obtained from a matrix isolation study of the photolysis of GeH_4 in 1972,[15] were for many years the only experimental data available on the parent molecule. More detailed information was provided throughout the 1990s from laser-induced fluorescence and microwave spectroscopies, and photoionization mass spectrometry.[16–20] Several detailed kinetic studies of the reactivity of GeH_2 have been reported, following the first such study in 1996.[21–30] Some experimental data for dimethylgermylene have also been reported (see Ref. 2 and references cited therein), such as its UV–Vis absorption,[31,32] IR,[33] and mass[34] spectra.

*Correspondence to: Anna Chrostowska, Laboratoire de Physico-Chimie Moléculaire, UMR 5624, Université de Pau, Av. de l'Université, BP 1155, 64013 Pau Cedex, france.
E-mail: anna.chrostowska@univ-pau.fr
**Correspondence to: William J. Leigh, Department of Chemistry, McMaster University, 1280 Main Street West, Hamilton, Ontario L8S 4M1, Canada.
E-mail: leigh@mcmaster.ca
†Based on work presented at the Sixth International Conference on Environmental and Biological Aspects of Main-group Organometals, Pau, France, 3–5 December 2003.
Contract/grant sponsor: Natural Sciences and Engineering Research Council of Canada.
Contract/grant sponsor: Conseil Régional d'Aquitaine.

In this study, we describe the results of flash vacuum thermolysis (FVT) of the simple 3,4-dimethyl-1-germacyclopent-3-ene derivatives **1**–**3**, in which the products (both stable and transient) have been detected in the gas phase and characterized by UV photoelectron spectroscopy (PES; Scheme 1). Compounds of this type (including **2**) are known to undergo formal 4 + 1 cheletropic elimination to yield the corresponding germylene and 1,3-diene upon pyrolysis in the gas phase,[35] and have been shown to be efficient and useful precursors of other germylene derivatives in previous transient FVT-PES studies in the Pau laboratories.[36–38] They are particularly convenient for such studies because of their moderate volatility, good stability under high-vacuum conditions, and the relative ease with which they can be synthesized, purified, and handled. Furthermore, the PE spectrum of the thermolysis co-product (2,3-dimethyl-1,3-butadiene (DMB)) is both relatively simple and quite distinctive,[39,40] which allows the course of thermolysis to be easily monitored and simplifies spectral interpretation. The FVT-PES technique is a powerful aid to our understanding of the electronic structures of transient molecules. Unfortunately, the interpretation of the PE spectra is not straightforward; so, theoretical evaluation of ionization potentials (IPs) is necessary for a reliable assignment. This has been carried out using time-dependent density functional theory (TD-DFT) methods, the results of which are compared with those estimated by outer valence Green's function (OVGF) calculations and the less rigorous 'shifting' of calculated Kohn–Sham energies.

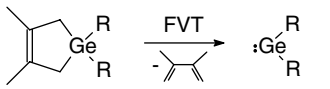

1 R=H, **2** R=Me, **3** R=Ph — **4** R=H, **5** R=Me, **6** R=Ph

Scheme 1.

EXPERIMENTAL RESULTS

Photoelectron spectra

The UV PE spectra of 3,4-dimethylgermacyclopent-3-ene (**1**), 1,1,3,4-tetramethylgermacyclopent-3-ene (**2**) and 3,4-dimethyl-1,1-diphenylgermacyclopent-3-ene (**3**) are shown in Fig. 1. The PE spectrum of **1** (Fig. 1a) exhibits three well-resolved bands at 8.5, 9.9 and 10.7 eV, followed by a broad band at 12.3 eV with a shoulder at 11.75 eV. The PE spectrum of **2** (Fig. 1b) displays the first ionization at 8.3 eV, then three well-distinguished ionizations at 9.5, 10.1 and 10.4 eV. The third precursor (**3**; Fig. 1c) shows a first broad ionization at 8.2 eV, followed by an intense band at 9.0 eV with shoulders at 8.6 and 9.2 eV, and a second broad band containing three ionizations at 9.6, 9.9 and 10.1 eV.

The three compounds were pyrolyzed in the inlet of the PE spectrometer at the temperatures necessary for partial thermolysis, as evidenced by the appearance of the characteristic spectrum of 2,3-dimethyl-1,3-butadiene in that of the thermolysate: 380 °C for **1**, 600 °C for **2**, and 470–820 °C for **3**. The resulting spectra are shown in Figs 2–4.

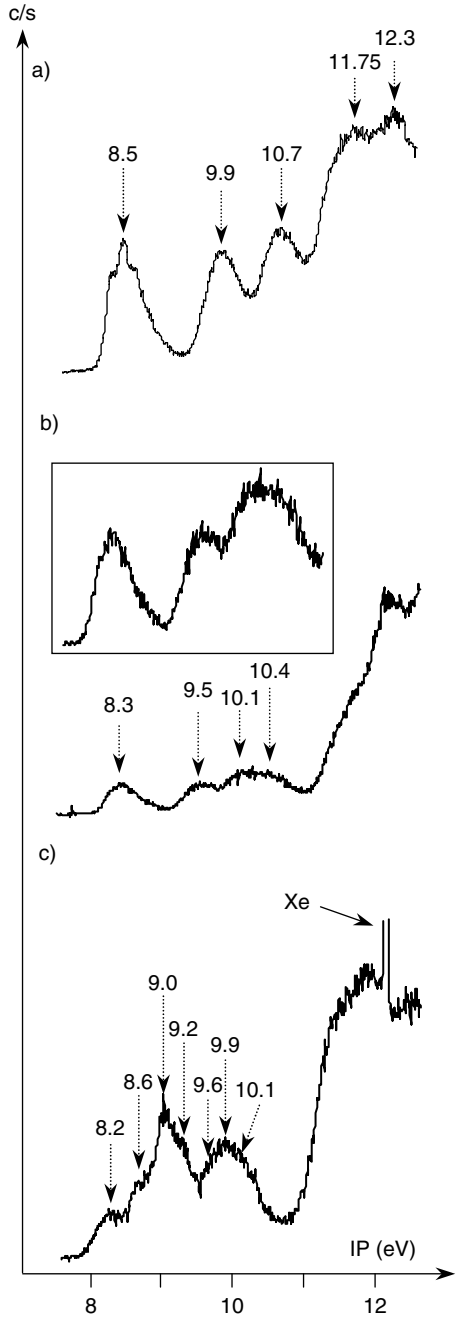

Figure 1. PE spectra of (a) **1**, (b) **2** and (c) **3**.

Starting from 380 °C (Fig. 2 curve a), the spectrum of precursor **1** has changed; the ionization bands due to DMB at 8.7, 8.9 and 9.2 eV have appeared (Fig. 2, curve b), and the presence of the band at 8.5 eV due to **1** (Fig. 2, curve c) confirms that thermolysis is not complete. The thermolysis spectrum also clearly shows a new band centered at 9.4 eV.

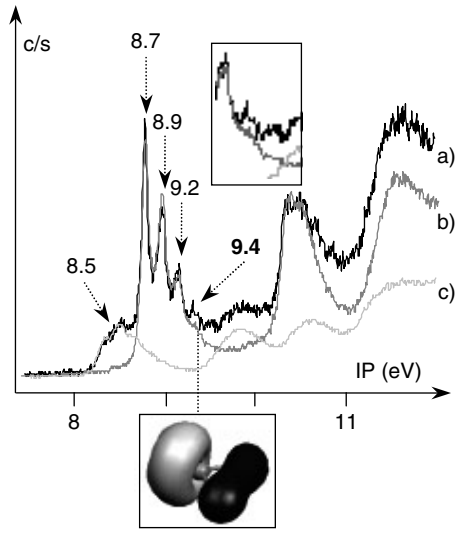

Figure 2. PE spectra of (a) **1** at 380 °C, (b) DMB, (c) **1** at 150 °C and Molekel visualization of the highest occupied molecular orbital of GeH_2.

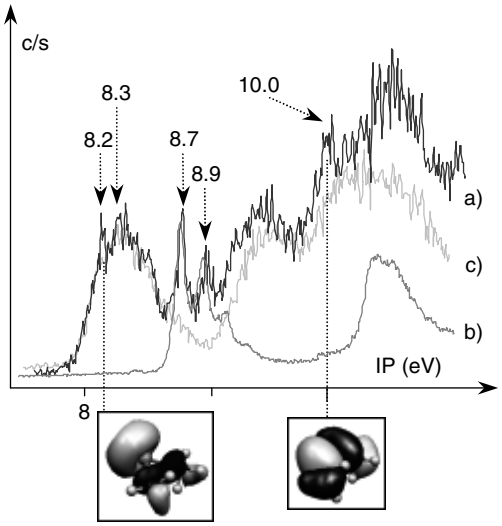

Figure 3. PE spectra of (a) **2** at 600 °C, (b) DMB, (c) **2** at 245 °C and Molekel visualization of the highest and second-highest molecular orbitals of $GeMe_2$.

Similarly, thermolysis of **2** at 600 °C leads to the appearance of new ionizations at 8.2 and 10.0 eV, while the FVT efficiency is confirmed by the presence of ionizations due to DMB (Fig. 3, curve b) and the precursor (Fig. 3, curve c). For these two compounds, the spectra recorded with thermolysis temperatures in excess of 380 °C and 600 °C respectively contain only the well-distinguished bands corresponding to DMB ionizations.

In the case of the putative diphenylgermylene precursor **3**, thermolysis at 470 °C led to the appearance of ionizations due to DMB superimposed on those due to the precursor; the latter were reduced in intensity compared with the spectrum recorded at lower temperatures (Fig. 4). No new ionizations other than those due to DMB could be distinguished in the spectrum, but changes in the intensity and shape of the lowest energy band centered at 8.2 eV are clearly evident. Heating at 630 °C and higher resulted in the appearance of a single new band at 9.24 eV, which is assigned to benzene.[41] With a thermolysis temperature of 820 °C, the PE spectra of this compound consisted only of ionizations due to DMB and benzene.

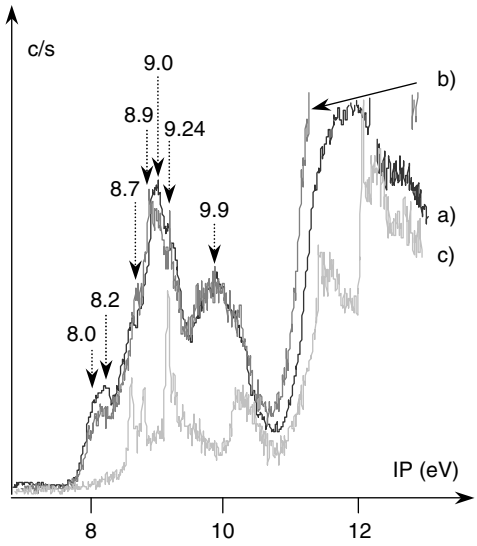

Figure 4. PE spectra of **3** at (a) 470 °C, (b) 630 °C and (c) 875 °C.

Theoretical results and UV photoelectron spectral interpretations: germacyclopentenes 1–3

The optimized (B3LYP/6-311G(d,p)) geometrical parameters for the three germacyclopentene derivatives are listed in Table 1. The germacyclopentenyl rings are predicted to be planar in all three cases. In the case of **1**, the calculated Ge–H bond distance is slightly longer and the H–Ge–H bond angle is 0.8° smaller than the experimentally determined values for GeH_4 (Ge–H 1.525 Å, H–Ge–H 109.5°).[42] For **2** and **3**, all calculated ring-framework bond lengths agree to within 0.03 Å with the corresponding experimental values for 1,1-dimethylgermacyclopent-3-ene, determined by gas-phase electron diffraction[43]. We note that the intra-annular Ge–C bond lengths in each of these structures are uniformly smaller than the extra-annular ones; and similarly, the C–Ge–C extra-annular bond angles are characteristically larger than the intra-annular C–Ge–C ones. Variation of the substituents on the germanium atom causes only small changes in the geometrical parameters associated with the basic structure of the molecule, as would be expected.

Table 1. Calculated (B3LYP/6-311G(d,p)) geometrical parameters (distances Å and angles (°)) for **1, 2** and **3**

	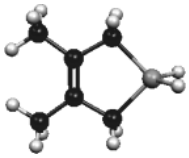 **1** C_{2v}	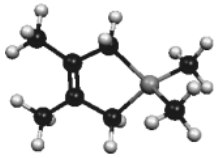 **2** C_{2v}	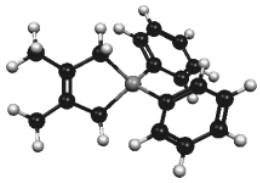 **3** C_2
Ge–H (1)	1.540		
Ge–C(Me) (2)		1.973	
Ge–C(Ph) (3)			1.970
Ge–C(ring)	1.976	1.981	1.981
C–C(ring)	1.522	1.521	1.520
C=C	1.348	1.349	1.348
H–Ge–H (1)	108.7		
C–Ge–C (Me) (2)		110.1	
C–Ge–C(Ph) (3)			110.1
C–Ge–C (ring)	92.3	91.8	91.8

Table 2. Comparison of calculated and experimental IPs for **1**

Exp. IP (eV)	Nature of MO	−KS energy (eV)	Estimated IP (eV)	TD-DFT IP (eV)	OVGF IP (eV)
8.5	$\pi_{C=C}(B_1)$	6.29	8.5[a]	8.34[b]	8.40
9.9	$\sigma^{-}_{Ge-C}(B_2)$	7.59	9.80	9.28	9.72
10.7	$\sigma^{+}_{Ge-C}(A_1)$	8.30	10.51	9.91	10.61
11.75	$\sigma^{-}_{Ge-H}(B_1)$	8.79	11.00	10.16	11.54

[a] Experimental value.
[b] Value of ΔSCF.

Table 3. Comparison of calculated and experimental IPs for **2**

Exp. IP (eV)	Nature of MO	−KS energy (eV)	Estimated IP (eV)	TD-DFT IP (eV)	OVGF IP (eV)
8.3	$\pi_{C=C}(B_1)$	6.12	8.30[a]	8.10[b]	8.20
9.5	$\sigma^{-}_{Ge-C(cycle)}(B_2)$	7.19	9.37	8.76	9.26
10.1	$\sigma^{+}_{Ge-C(cycle)}(A_1)$, $\sigma^{+}_{Ge-C(Me)}(A_1)$	7.72	9.90	9.00	9.84
10.4	$\sigma^{-}_{Ge-C(Me)}(B_1)$	7.90	10.08	9.10	10.16

[a] Experimental value.
[b] Value of ΔSCF.

The evaluation of ionization potentials has been carried out using TD-DFT[44,45] and OVGF[46,47] calculations on the optimized structures, as well as by the more commonly employed method involving 'shifting' of the B3LYP/6-311G(d,p) Kohn–Sham energies.[48–50] Comparisons with experimental data for previously studied sila- and germacyclopentenes[51–53] also proved valuable. Comparisons between the calculated, estimated, and experimental IPs for **1** (Table 2), **2** (Table 3) and **3** (Table 4) allowed assignment of the lowest energy ionizations, which are fairly well separated from the rest of the bands in the spectra of **1**–**3**, to the C–C π molecular orbital (MO) at 8.5 eV, 8.3 eV and 8.2 eV respectively.

Table 4. Comparison of calculated and experimental IPs for **3**

Exp. IP (eV)	Nature of MO	−KS energy (eV)	Estimated IP (eV)	TD-DFT IP (eV)
8.2	$\pi_{C=C}$ (B)	6.18	8.2[a]	7.98[b]
8.6	Ph (B)	6.65	8.67	8.20
	Ph (B)	6.95	8.97	8.21
9.0–9.2	Ph (A)	6.97	8.99	8.42
	Ph (B)	7.02	9.04	9.23
9.6	$\sigma^{-}_{Ge-C(cycle)}$ (B)	7.76	9.78	9.41
9.9	$\sigma^{+}_{Ge-C(Ph)}$ (A)	7.92	9.94	9.415

[a] Experimental value.
[b] Value of ΔSCF.

The higher energy ionization bands in the spectra of **1**–**3** correspond mainly to the antibonding and bonding combinations associated with the intra-annular Ge–C bonds in the case of **1** (9.9, 10.7 eV), and with those due to both the intra- and extra-annular Ge–C bonds in the cases of **2** (9.5, 10.1, 10.4 eV) and **3** (9.6, 9.9, 10.1 eV). In the spectrum of **3**, the intense band at 9.0 eV with shoulders at 8.6 and 9.2 eV is assigned to ionizations involving MOs localized on the phenyl rings. We note that methyl or phenyl disubstitution on the gomanium atom in 3,4-dimethylgermacyclopentene causes a global lowering of all the IPs except the second one, which is

stabilized by *ca* 0.1 eV in the case of **3** compared with **2**. Of course, the opposite effect is observed in germacyclopentenes bearing electron-withdrawing substituents (e.g. chlorine) at the germanium atom (8.87 (b_1), 9.96 (b_2), 11.3 eV (b_1); Laporte-Chrostowska A, Lemierre V, unpublished results). As has been mentioned above (see Table 1), the calculated geometrical parameters (Ge–C bond lengths and C–Ge–C intra- and extra-annular bond angles) vary only slightly as a function of substituent at germanium in 1–3, so the dominant factor responsible for the observed variations in the IPs throughout the series is the electronic effects of the substituents. The same trend has been observed in the PE spectra of silacyclopent-3-ene derivatives, in which the substitution of germanium by silicon causes a slight, but fairly uniform, stabilization of all the IPs relative to those of the corresponding germacyclopent-3-enes.[51–53] The excellent agreement between OVGF and experimental values of IPs for **1** and **2** should be noted (we have not been successful in our attempts to obtain IPs for **3** by this theoretical method because of the large size of this molecule), and they agree surprisingly well with the IPs estimated from shifting of the B3LYP/6-311G(d,p) MO energies. The TD-DFT method characteristically underestimates the IPs of the three precursor molecules, which is most likely due to inadequacies in the evaluation of the first ionic state.

GeH_2, $GeMe_2$, and $GePh_2$

Several theoretical studies concerning GeH_2,[3] $GeMe_2$,[3] and $GePh_2$[54] have been reported, and the results of calculations at the various levels of theory employed were compared with experimental data available for GeH_2[19] and bis[2,6-bis(1-naphthyl)phenyl]germylene [Ge(bisap)$_2$][54]. Evaluation of the germylene IPs in the present study has been carried out after B3LYP/6-311G(d,p) geometry optimization of the lowest lying $^1A_1$ states (data not shown, but in reasonable agreement with those reported previously for GeH_2,[11–13] $GeMe_2$,[11,12] and $GePh_2$[54]). The results of the calculations are compared with the experimentally determined values, and the estimates obtained by shifting of the calculated Kohn–Sham energies, in Tables 5–7. The lowest IPs reported here for GeH_2 and $GeMe_2$ agree well with the previously calculated values of Trinquier and coworkers (9.05 eV for the non-bonding σ orbital in GeH_2 and 8.12 eV for that in $GeMe_2$),[10] and with the upper limit of 9.25 eV for the lowest adiabatic IP of GeH_2 determined by Berkowitz and coworkers by photoionization mass spectrometry.[16] The 0.15 eV difference between the adiabatic and the vertical IPs is due to differences between the structures of the ion states populated in the adiabatic and vertical ionizations; our calculations indicate that the H–Ge–H bond angle and Ge–H distances are respectively 12.4° and 0.018 Å larger in the relaxed radical cation compared to the corresponding values in the ground-state structure.

We thus assign the ionization band at 9.4 eV in the spectrum of the thermolysate from **1** (Table 5) to the ejection of an electron from the germanium lone pair (n_{Ge}) in GeH_2. Ionizations corresponding to the antibonding and bonding combination of σ_{Ge-H} bonds are calculated at 11.2–11.4 eV and 16.6–17 eV respectively; but, as these are superimposed on ionizations due to DMB and **1**, they cannot be distinguished in the experimental spectra. In the corresponding spectrum from **2**, the first band at 8.2 eV is associated with the n_{Ge} orbital in $GeMe_2$. The calculations suggest that the second band observed at 10.0 eV corresponds to the ejection of an electron from the σ^-_{Ge-C} orbital. IPs calculated to lie above 12.6 eV cannot be distinguished in the spectrum owing to interference from bands due to DMB and the precursor, **2**.

According to the IP calculations for $GePh_2$ (Table 7), the first band corresponding to ionization of a germylene lone-pair electron is expected at *ca* 8.0 eV, and should be followed by higher energy bands at 9.0–9.2 eV and *ca* 9.8 eV that originate in benzenoid and σ^-_{Ge-C} MOs respectively. The 470 °C FVT-PES spectrum of **3** shows clear evidence of ionizations due to DMB, suggesting that cheletropic elimination

Table 5. Comparison of calculated and experimental IPs for **4**

Exp. IP	Nature of MO	−KS energy (eV)	Estimated IP (eV)	TD-DFT IP (eV)	OVGF IP (eV)
9.4	$n_{Ge}(A_1)$	6.77	9.4[a]	9.54[b]	9.23
	$\sigma^-_{Ge-H}(B_2)$	8.63	11.26	11.44	11.43
	$\sigma^+_{Ge-H}(A_1)$	14.20	16.83	16.65	17.06

[a] Experimental value.
[b] Value of ΔSCF.

Table 6. Comparison of calculated and experimental IPs for **5**

Exp. IP (eV)	Nature of MO	−KS energy (eV)	Estimated IP (eV)	TD-DFT IP (eV)	OVGF IP (eV)
8.2	n_{Ge} (A)	−5.92	8.20[a]	8.29[b]	8.12
10.0	σ^-_{Ge-C} (B)	−7.76	10.04	10.07	10.17
	$\sigma^-_{C-H(\sigma)}$ (B)	−10.59	12.87	12.59	13.63
	$\sigma^-_{C-H(\pi)}$ (A)	−10.62	12.90	12.61	13.63

[a] Experimental value.
[b] Value of ΔSCF.

Table 7. Comparison of calculated and experimental IPs for **6**

Estimated exp. IP (eV)	Nature of MO	−KS energy (eV)	OVGF IP (eV)	TD-DFT IP (eV)
8.0–8.2	n_{Ge} (A)	5.96	7.79	7.75[a]
9.0–9.2	Ph.(B, A, A, B)	7.06–7.26	8.82–9.04	8.40, 8.42, 8.61, 8.71
9.8–10.0	σ^-_{Ge-C} (B)	7.81	9.67	9.44

[a] Value of ΔSCF.

of $GePh_2$ occurs as planned at this temperature. Nevertheless, the changes evident in the 470 °C spectrum compared to that of the precursor are too minor to make unambiguous assertions as to their origins. The appearance of the characteristic ionizations due to benzene, which are evident in spectra recorded at higher thermolysis temperatures (>630 °C), suggests the intervention of additional, higher energy decomposition pathways, perhaps involving the formation of 3,4-dimethyl-1-germacyclopent-3-ene-1,1-diyl (**7**) and/or its principal isomerization product, 3,4-dimethyl-1*H*-germole (**8**), via consecutive hydrogen shifts as previously evidenced by Khabashesku *et al*.[55] (Scheme 2). B3LYP/6-311(d,p) calculations indicate that the lowest energy ionizations for **7** and **8** can be expected at 8.2 eV and 8.14 eV respectively; so, evidence for their formation is no easier to obtain than that for formation of $GePh_2$ from the experimental spectra. Total decomposition of **3** occurs at temperatures above 820 °C, but the only distinguishable bands are due to DMB and benzene.

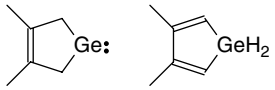

7 **8**

Scheme 2.

IPs corresponding to the germanium lone pair decrease in energy upon dimethyl substitution at germanium, from 9.4 eV in the case of GeH_2 to 8.2 eV for $GeMe_2$, which compares with the theoretical estimate of 8.0–8.2 eV for the lowest energy ionization in $GePh_2$. This trend can be explained as being mainly due to the increasing bond angle about germanium throughout the series: 90.69° for H–Ge–H,[11] 95.5° for the C–Ge–C[11] bond angle in $GeMe_2$ and 101.6° for that in $GePh_2$.[54] The largest destabilization of the σ_{Ge} MO, based on these considerations, is expected for $GePh_2$, but the effect is compensated for by the inductive electron-withdrawing effect of the phenyl substituents. The trend toward decreasing σ_{Ge} IP with increasing bond angle about germanium is further reflected in the lowest energy IP (7.75 eV)[56a] of the stable homoleptic alkylgermylene :Ge[$CH(SiMe_3)_2$], for which the C–Ge–C bond angle (107.2°) is known from gas-phase electron diffraction data.[56b] This and the less pronounced inductive electron-withdrawing effect of the two $CH(SiMe_3)_2$ groups, compared with phenyl, combine to destabilize the σ_{Ge} MO in this germylene to a much greater extent than is predicted for $GePh_2$.

Conclusions

The FVT-PES method has allowed, for the first time, the measurement of the lowest vertical ionization bands for GeH_2 (9.4 eV) and $GeMe_2$ (8.2 and 10.0 eV), generated by thermal cheletropic elimination from 3,4-dimethylgermacyclopent-3-ene (**1**) and 1,1,3,4-tetramethylgermacyclopent-3-ene (**2**) over very narrow temperature intervals. The PE spectrum of diphenylgermylene ($GePh_2$) is most likely obscured by the bands corresponding to the precursor (**3**), but the spectrum is nevertheless consistent with the theoretically predicted lowest IP of 8.0–8.2 eV. The variation in the lowest energy IPs of the three simple germylene derivatives studied here is thought to be due mainly to the differences in the bond angles at germanium, with additional perturbations due to variations in the electronic effects of the substituents.

Quite good agreement between theoretical and experimental IP data for the germylenes is observed, but TD-DFT (B3LYP/6-311G**) calculations on the precursors indicate that the method is less satisfactory than the OVGF method for these (stable) molecules. Those aspects of the electronic structures of the substituted 3,4-dimethylgermacyclopent-3-enes (**1**–**3**) that are probed by UV-PES methods are in fairly close correspondence to those of the analogous silicon compounds.

EXPERIMENTAL

Preparation of compounds

^1H and ^{13}C NMR spectra were recorded in chloroform-*d* using a Bruker AV200 spectrometer, and are referenced to tetramethylsilane. Diethyl ether (BDH Omnisolv) and tetrahydrofuran (THF; Caledon Reagent) were dried by passage through columns of activated alumina. Germanium tetrachloride was used as received from Gelest Inc., and other materials were used as received from Aldrich, Inc. All synthetic preparations were carried out under an atmosphere of dry nitrogen.

Germanium dichloride–dioxane and 1,1-dichloro-3,4-dimethylgermacyclopent-3-ene (**9**) were prepared by the procedures of Nefedov and coworkers,[54] with minor modifications. For the former, a mixture of germanium tetrachloride (25.0 g, 0.117 mol), 1,1,3,3-tetramethyldisiloxane (17.3 g, 0.129 mol) and 1,4-dioxane (18.0 g, 0.205 mol) were heated under nitrogen to 85 °C over 1 h, and then left at this temperature for a further 12 h. The resulting suspension of colorless crystals was cooled and the excess solution was decanted off. The crystals were washed with pentane to yield $GeCl_2$–dioxane as colorless needles (21.9 g, 0.095 mol, 81%, m.p. 100–150 °C).[57] For the preparation of **9**, $GeCl_2$–dioxane (5.0 g, 21.5 mmol) and dry THF (100 ml) were heated to reflux with stirring under nitrogen, and then a solution of 2,3-dimethyl-1,3-butadiene (2.3 g, 33.8 mmol) in dry THF (20 ml) was added dropwise over 1 h. The solution was stirred for a further 10 min, the apparatus was reconfigured for distillation, and the solvent was distilled off under nitrogen. Continued distillation under vacuum afforded **9** (4.29 g, 18.9 mmol, 88%) as a colorless liquid (b.p. 35–37 °C, 0.1 mmHg (lit.[58] 120 °C, 26 mmHg)). ^1H NMR, δ: 1.80 (s, 6H), 2.22 (s, 4H); ^{13}C NMR, δ: 18.7, 32.9, 129.2.

*3,4-Dimethylgermacyclopent-3-ene (**1**)*

To a slurry of lithium aluminum hydride (1.0 g, 27 mmol) in 100 ml anhydrous Et_2O at −78 °C (acetone/CO_2) was added **9**

(5.30 g, 23.3 mmol) over 5 min, and the reaction was warmed to room temperature and stirred for 12 h. The organic layer was decanted off and hydrolyzed with water (*ca* 10 ml). The layers were separated, the ethereal layer was dried over anhydrous magnesium sulfate, filtered, and the solvent was then removed on a rotary evaporator to yield a colorless oil. Vacuum distillation afforded 3.16 g (20.0 mmol, 87%) of 3,4-dimethyl-1-germacyclopent-3-ene (**1**; b.p. 25 °C, 4 mmHg (lit.[58] 142 °C, 760 mmHg)). ^{1}H NMR, δ: 1.73 (s, 6H), 1.79 (bs, 4H), 3.93 (q, 3.4 Hz, 2H); ^{13}C NMR, δ: 19.1, 20.7, 131.1.

*1,1,3,4-Tetramethylgermacyclopent-3-ene (**2**)*

To a solution of **9** (4.20 g, 18.5 mmol) in anhydrous THF (75 ml) at 5 °C was added a solution of methylmagnesium bromide (13.5 ml of a 3.0 M solution in Et_2O, 40.5 mmol) in anhydrous THF (25 ml), and the resulting mixture was stirred at room temperature for 24 h. After hydrolysis, extraction of the organic layer (Et_2O), and drying with magnesium sulfate, the solvent was removed on a rotary evaporator to yield a light-yellow oil. Vacuum distillation afforded the product (3.24 g, 17.4 mmol, 94%) as a colorless liquid (b.p. 45 °C, 4 mmHg (lit.[58] 71 °C, 27 mmHg)). The compound exhibited NMR data similar to those previously reported.[59] ^{1}H NMR ($CDCl_3$), δ: 0.29 (s, 6H), 1.52 (s, 4H), 1.71 (s, 6H); ^{13}C NMR δ: −2.5, 19.4, 26.9, 130.9.

*3,4-Dimethyl-1,1-diphenylgermacyclopent-3-ene (**3**)*

To a solution of **9** (5.00 g, 22.1 mmol) in anhydrous THF (100 ml) at 5 °C was added a solution of phenylmagnesium bromide (18.5 ml of a 3.0 M solution in Et_2O, 55.5 mmol) in anhydrous THF (25 ml), and the resulting mixture was stirred at room temperature for 24 h. After hydrolysis, extraction of the organic layer (Et_2O), and drying over magnesium sulfate, the solvent was removed on a rotary evaporator to yield a light-yellow oil (5.3 g) that solidified upon cooling to *ca* −20 °C. The solid was recrystallized slowly, once from 1 : 1 (v/v) acetone–isopropanol and then repeatedly from 1 : 3 (v/v) acetone–hexane, with gas chromatography analysis in between, until <0.01% biphenyl remained (usually three or four slow recrystallizations). The product was finally obtained as colorless crystals (4.06 g, 13.1 mmol, 59%; m.p. 48.6–49.3 °C (lit.[58] 40–41 °C)), whose ^{1}H NMR spectrum agreed well with that previously reported.[59] ^{1}H NMR ($CDCl_3$), δ: 1.82 (s, 6H), 2.05 (s, 4H), 7.39 (m, 6H), 7.56 (m, 4H); ^{13}C NMR, δ: 19.5, 25.7, 128.3, 128.9, 130.9, 134.3, 138.5.

UV photoelectron spectra

The PE spectra were recorded on a home-built, three-part spectrometer equipped with a spherical analyzer (Omicron), main body device (Meca2000), He I radiation source (Focus), and monitored by a microcomputer supplemented with a digital–analog converter. The spectra were calibrated against the auto-ionization of xenon at 12.13 and 13.45 eV, and nitrogen at 15.59 and 16.98 eV. Sample manipulations were carried out in a thermolysis oven attached directly to the inlet probe; the distance between the oven exit and the ionization head does not exceed 1 cm. Compounds **1**–**3** were slowly vaporized under low pressure (10^{-7} Torr in the ionization chamber) directly in the oven, and the gaseous thermolysate was continuously analyzed.

Computational methods

The calculations were performed using the Gaussian 98[60] program package using the DFT[61,62] method. Geometry optimizations were carried out at the B3LYP/6-311G(d,p) level of theory,[63–65] and were followed by frequency calculations in order to verify that the stationary points obtained were true energy minima. The hybrid gradient-corrected exchange functional proposed by Becke combined with the gradient-corrected correlation functional of Lee, Yang and Parr has been shown to be quite reliable for geometries of germanium-containing compounds.[38]

To calculate the first ionic states, TD-DFT was used. This calculation is based on the evaluation of the electronic spectrum of the low-lying ion, described by the ΔSCF corresponding to the first vertical IP, i.e. IP_{1v}^{cal}, calculated as the difference $E_{cation} - E_{neutral\,molecule}$. The vertical IPs were also calculated at the *ab initio* level by employing the OVGF method, which includes electron correlation and electron relaxation effects.[46,47] So-called 'estimated IPs' were calculated by applying a uniform shift ($x = |-^{KS}(HOMO) - IP_v^{exp}|$, where ^{KS}(HOMO) is the highest occupied B3LYP/3-111G(d,g) Kohn–Sham MO energy of the ground-state molecule and IP_v^{exp} is the lowest energy experimental IP of the molecule. Stowasser and Hoffman[66] have recently shown that the localized Kohn–Sham orbitals are very similar to those obtained from Harfree–Fock calculations, so it is possible to determine the nature of the first ionizations and to interpret the PE spectra unambiguously.

Acknowledgements

WJL and CRH are grateful to the Natural Sciences and Engineering Research Council of Canada for financial support. AC and VL acknowledge the Conseil Régional d'Aquitaine for financial support for VL.

REFERENCES

1. Gaspar PP, West R. In *The Chemistry of Organic Silicon Compounds*, Vol. 2, Rappoport Z, Apeloig Y (eds). John Wiley: Chichester, 1998; chapter 43.
2. Boganov SE, Egorov MP, Faustov VI, Nefedov OM. In *The Chemistry of Organic Germanium, Tin and Lead Compounds*, Vol. 2, Rappoport Z (ed.). John Wiley: Chichester, 2002; chapter 12.
3. Neumann WP. *Chem. Rev.* 1991; **91**: 311.
4. Driess M, Grützmacher H. *Angew. Chem. Int. Ed. Engl.* 1996; **35**: 828.
5. Barrau J, Rima G. *Coord. Chem. Rev.* 1998; **178–180**: 593.
6. West R, Denk M. *Pure Appl. Chem.* 1996; **68**: 785.
7. Denk M, West R, Hayashi R, Apeloig Y, Pauncz R, Karni M. In *Organosilicon Chemistry II*, Auner N, Weis J (eds). VCH: Weinheim, 1996.
8. Tokitoh N, Okazaki R. *Coord. Chem. Rev.* 2000; **210**: 251, 2333.
9. Olbrich G. *Chem. Phys. Lett.* 1980; **73**: 110.

10. Barthelat JC, Saint Roch B, Trinquier G, Satgé J. *J. Am. Chem. Soc.* 1980; **102**: 4080.
11. Su MD, Chu SY. *J. Am. Chem. Soc.* 1999; **121**: 4229.
12. BelBruno JJ. *Heteroat. Chem.* 1998; **9**: 195.
13. Szabados A, Hargittai M. *J. Phys. Chem. A* 2003; **107**: 4314.
14. Apeloig Y, Pauncz R, Karni M, West R, Steiner W, Chapman D. *Organometallics* 2003; **22**: 3250.
15. Smith R, Guillory WA. *J. Chem. Phys.* 1972; **56**: 1423.
16. Ruscic B, Schwarz M, Berkowitz J. *J. Chem. Phys.* 1990; **92**: 1865.
17. Saito K, Obi K. *Chem. Phys. Lett.* 1993; **215**: 193.
18. Saito K, Obi K. *Chem. Phys* 1994; **187**: 381.
19. Karolczak J, Harper WW, Grev RS, Clouthier DJ. *J. Chem. Phys.* 1995; **103**: 2839.
20. Smith R, Clouthier DJ, Sha W, Adam AG. *J. Chem. Phys.* 2000; **113**: 9567.
21. Becerra R, Boganov SE, Egorov MP, Nefedov OM, Walsh R. *Chem. Phys. Lett.* 1996; **260**: 433.
22. Becerra R, Boganov SE, Egorov MP, Faustov VI, Nefedov OM, Walsh R. *J. Am. Chem. Soc.* 1998; **120**: 12 657.
23. Alexander UN, Trout NA, King KD, Lawrance WD. *Chem. Phys. Lett.* 1999; **299**: 291.
24. Becerra R, Walsh R. *Phys. Chem. Chem. Phys.* 1999; **1**: 5301.
25. Alexander UN, King KD, Lawrance WD. *Chem. Phys. Lett.* 2000; **319**: 529.
26. Becerra R, Boganov SE, Egorov MP, Faustov VI, Nefedov OM, Walsh R. *Can. J. Chem.* 2000; **78**: 1428.
27. Becerra R, Boganov SE, Egorov MP, Faustov VI, Nefedov OM, Walsh R. *Phys. Chem. Chem. Phys.* 2001; **3**: 184.
28. Becerra R, Walsh R. *J. Organometal. Chem.* 2001; **636**: 49.
29. Becerra R, Walsh R. *Phys. Chem. Chem. Phys.* 2002; **4**: 6001.
30. Becerra R, Boganov SE, Egorov MP, Faustov VI, Promyslov VM, Nefedov OM, Walsh R. *Phys. Chem. Chem. Phys.* 2002; **4**: 5079.
31. Ando W, Tsumuraya T, Sekigushi A. *Chem. Lett.* 1987; 317.
32. Becerra R, Boganov SE, Egorov MP, Lee VYa, Nefedov OM, Walsh R. *Chem. Phys. Lett.* 1996; **250**: 111.
33. Barrau J, Bean DL, Welsh KM, West R, Michl J. *Organometallics* 1989; **8**: 2606.
34. Duffield AM, Djerassi C, Mazerolles P, Dubac J, Manuel G. *J. Organometal. Chem.* 1968; **12**: 123.
35. Lei D, Gaspar PP. *Polyhedron* 1991; **10**: 1221.
36. Laporte-Chrostowska A, Foucat S, Pigot T, Lemierre V, Pfister-Guillouzo G. *Main Group Met. Chem.* 2002; **25**: 55.
37. Chrostowska A, Lemierre V, Pigot T, Pfister-Guillouzo G, Saur I, Miqueu K, Rima G, Barrau J. *Main Group Met. Chem.* 2002; **25**: 69.
38. Saur I, Miqueu K, Rima G, Barrau G, Lemierre V, Chrostowska A, Sotiropoulos JM, Pfister-Guillouzo G. *Organometallics* 2003; **22**: 3143.
39. Sustmann R, Schubert R. *Tetrahedron Lett.* 1972; 2739.
40. Beez M, Bieri G, Bock H, Heilbronner E. *Helv. Chim. Acta* 1973; **56**: 1028.
41. Kimura K, Katsumata S, Achiba Y, Yamazaki T, Iwata S. *Handbook of HeI Photoelectron Spectra of Fundamental Organic Molecules*, Part II. Japan Scientific Societies Press/Halsted Press: Tokyo/New York, 1981; 188.
42. Patai S. *The Chemistry of Organic Germanium, Tin and Lead Compounds*. John Wiley: Chichester, 1995; 101.
43. Aarset K, Page EM, Rice DA. *J. Phys. Chem. A* 1999; **103**: 5574.
44. Stratmann RE, Scuseria GE, Frisch MJ. *J. Chem. Phys.* 1998; **109**: 8218.
45. Casida ME, Jamorski C, Casida KC, Salahub DR. *J. Chem. Phys.* 1998; **108**: 4439.
46. Von Niessen W, Schirmer J, Cederbaum LS. *Comput. Phys. Rep.* 1984; **1**: 57.
47. Ortiz JV. *J. Chem. Phys.* 1988; **89**: 6348.
48. Arduengo AJ, Bock H, Chen H, Denk M, Dixon DA, Green JC, Hermann WA, Jones NL, Wagner M, West R. *J. Am. Chem. Soc.* 1994; **116**: 6641.
49. Muchall H, Werstiuk N, Pitters J, Workentin M. *Tetrahedron* 1999; **55**: 3767.
50. Chrostowska A, Dargelos A, Lemierre V, Sotiropoulos JM, Guenot P, Guillemin JC. *Angew. Chem. Int. Ed. Engl.* 2004; **43**: 873.
51. Schweig A, Weidner U, Manuel G. *Angew. Chem. Int. Ed. Engl.* 1972; **11**: 837.
52. Bertoti I, Cradock S, Ebsworth EAV, Whiteford RA. *J. Chem. Soc. Dalton Trans.* 1976; 937.
53. Guimon C, Pfister-Guillouzo G, Manuel G, Mazerolles P. *J. Organometal Chem.* 1978; **149**: 149.
54. Wegner GL, Berger RJF, Schier A, Schmidbaur H. *Organometallics* 2001; **20**: 418.
55. Khabashesku VN, Boganov SE, Antic D, Nefedov OM, Michl J. *Organometallics* 1996; **15**: 4714.
56. (a) Harris DH, Lappert MF, Pedley JB, Sharp GJ. *J. Chem. Soc. Dalton Trans.* 1976; 945; (b) Fjeldberg T, Haaland A, Schilling BER, Lappert MF, Thorne AJ. *J. Chem. Soc. Dalton Trans.* 1986; 1551.
57. Kolesnikov SP, Rogozhin IS, Nefedov OM. *Izv. Akad. Nauk SSSR Ser. Khim.* 1974; 2379.
58. Mazerolles P, Manuel G. *Bull. Soc. Chim. Fr.* 1966; 327.
59. Bobbitt KL, Maloney VM, Gaspar PP. *Organometallics* 1991; **10**: 2772.
60. Frisch MJ, Trucks GW, Schlegel HB, Scuseria GE, Robb MA, Cheeseman JR, Zakrzewski VG, Montgomery JA, Stratman RE, Burant JC, Dapprich S, Millam JM, Daniels AD, Kudin KN, Strain MC, Farkas O, Tomasi J, Barone V, Cossi M, Cammi R, Mennucci B, Pomelli C, Adamo C, Clifford S, Ochterski J, Petersson GA, Ayala PY, Cui Q, Morokuma K, Malick DK, Rabuck AD, Raghavachari K, Foresman JB, Cioslowski J, Ortiz JV, Baboul AG, Stefanov BB, Liu G, Liashenko A, Piskorz P, Komaromi I, Gomperts R, Martin R, Fox DJ, Keith DT, Al-Laham MA, Peng CY, Nanayakkara A, Gonzalez C, Challacombe M, Gill PMW, Jonhson B, Chen W, Wong MW, Andres JL, Head-Gordon M, Replogle ES, Pople JA. Gaussian 98, Revision A.7. Gaussian, Inc., Pittsburgh, PA, 1998.
61. Parr RG, Yang W. *Functional Theory of Atoms and Molecules*. Oxford University Press: New York, 1989.
62. Frish MJ, Trucks GW, Cheeseman JR. Systematic model chemistries based on density functional theory: comparison with traditional models and with experiment. In *Recent Development and Applications of Modern Density Functional Theory, Theoretical and Computational Chemistry*, vol. 4, Semminario JM (ed.). Elsevier: 1996; 79–707.
63. Becke AD. *Phys. Rev.* 1988; **38**: 3098.
64. Becke AD. *J. Chem. Phys.* 1993; **98**: 5648.
65. Lee C, Yang W, Parr RG. *Phys. Rev B.* 1988; **37**: 785.
66. Stowasser R, Hoffmann R. *J. Am. Chem. Soc.* 1999; **121**: 3414.

